

High-Precision Measurements of Brightness Variation of Nereid *

Tsuyoshi TERAII

National Astronomical Observatory of Japan, 2-21-1 Osawa, Mitaka, Tokyo 181-8588

tsuyoshi.terai@nao.ac.jp

and

Yoichi ITOH

Center for Astronomy, University of Hyogo, 407-2 Nishigaichi, Sayo-cho, Sayo-gun, Hyogo 679-5313

(Received 2012 August 16; accepted 2012 December 3)

Abstract

Nereid, a satellite of Neptune, has a highly eccentric prograde orbit with a semi-major axis larger than 200 Neptune radius and is classified as an irregular satellite. Although the capture origin of irregular satellites has been widely accepted, several previous studies suggest that Nereid was formed in the circumplanetary disk of Neptune and was ejected outward to the present location by Triton. Our time-series photometric observations confirm that the spin is stable and non-chaotic with a period of 11.5 hr as indicated by Grav et al. (2003). The optical colors of Nereid are indistinguishable from those of trans-Neptunian objects and Centaurs, especially those with neutral colors. We also find the consistency of Nereid's rotation with the size-rotation distribution of small outer bodies. It is more likely that Nereid originates in an immigrant body captured from a heliocentric orbit which was 4–5 AU away from Neptune's orbit.

Key words: Satellite — Nereid — Solar system: general

1. INTRODUCTION

NII Nereid is the second largest Neptunian satellite of 170 ± 25 km in radius (Thomas et al. 1991). It has a prograde orbit with a semi-major axis of 5.5×10^6 km and an eccentricity of 0.75 (Jacobson 2009). Because of its large and highly eccentric orbit, Nereid is categorized as an irregular satellite. Irregular satellites are generally believed to have been captured into the Hill sphere of the host planets from heliocentric orbits (e.g. Bailey 1971). However, as an

* Based on data collected at Subaru Telescope, which is operated by the National Astronomical Observatory of Japan (NAOJ).

exception, the history of Nereid is still unclear. Goldreich et al. (1989) suggest that Nereid could originally have been a regular satellite. In this model, it formed close to Neptune in the circumplanetary disk and then was transported outward due to perturbations by NI Triton. The orbit scattering could also change Nereid’s orbit from circular to eccentric.

Nereid is comparatively bright ($V \sim 19.2$ mag at opposition; Schaefer et al. 2008) for an irregular satellite. Numerous ground-based observations have been carried out for measuring the rotational properties. Some of them show large variations of the magnitude exceeding ~ 1.3 mag with a rotation period of 8–24 hr (Schaefer and Schaefer 1988; Williams et al. 1991). Schaefer and Schaefer (2000) argue that Nereid has a nonperiodic brightness variation with a total amplitude of 1.83 mag. We note that Nereid was located in vicinity of the galactic plane when these earlier data were collected and the apparent large variations could have been due to the crowded field stars. In contrast, Buratti et al. (1997) and Brown and Webster (1998) report a small amplitude of less than 0.1 mag. Also, measurements by Voyager 2 over a 12-day interval found no brightness variation greater than 0.15 mag (Thomas et al. 1991). Grav et al. (2003) performed relative photometry of Nereid with 0.003–0.006 mag accuracy using the CTIO 4-m telescope and obtained lightcurves with a peak-to-peak amplitude of 0.029 ± 0.003 mag and a rotation period of 11.52 ± 0.14 hr.

Different measurements so far report different levels of the rotational brightness variation. Schaefer and Schaefer (2000) suggest chaotic variations of the rotation from year to year, like SVII Hyperion (Klavetter 1989; Wisdom et al. 1984). Dobrovolskis (1995) propose that if Nereid was originally a regular satellite and has an elongated body with larger than $\sim 1\%$ of deviation from sphere, Nereid may be in chaotic rotation for any spin period of longer than about 2 weeks due to the tidal effect. On the other hand, the long-term variability of rotation is possibly produced by precession of the spin axis caused by the gravitational torques from Neptune (Schaefer et al. 2008; Alexander et al. 2011). While the possibility of chaotic rotation was excluded by Grav et al. (2003), the rotation state remains uncertain.

This paper presents time-series photometric data of Nereid collected at the 8.2-m Subaru Telescope. We determine the amplitude and period of the rotational brightness variation with high accuracy. They give strong indications of the rotation state of Nereid; whether stable or variable. In addition, the rotation period is available for investigating the links to other small bodies. We use the results to discuss the origin and dynamical evolution of Nereid in the final stage of planet formation.

2. OBSERVATIONS AND MEASUREMENTS

Observations were conducted on 2008 September 1, 2, and 29 UT using the Subaru Prime Focus Camera, Suprime-Cam (Miyazaki et al. 2002), mounted on the Subaru Telescope. The Suprime-Cam consists of ten 2048×4096 CCDs, which are arranged in a 5×2 pattern with interchip gaps of $\sim 15''$. It covers a $34' \times 27'$ field of view (FOV) with a pixel scale of $0''.20$.

Each image was obtained with a 240-sec exposure using the VR -band filter with the center wavelength of $0.6\ \mu\text{m}$ and the band width of $0.2\ \mu\text{m}$.

One FOV around Neptune was taken for 1–2 hours each night (Table 1). Neptune was placed at an interchip gap to reduce its bright light. Nereid was $\sim 7''$ away from Neptune and its solar phase angle shifted from 0.55° to 1.34° during our observations. The sky motion, $2.5\text{--}4.0\ \text{arcsec hr}^{-1}$, was slow enough to be approximately viewed as a point source within the exposure. The typical seeing was $0''.70$ in the first night, $0''.65$ in the second night, and $0''.60$ in the last night.

The data reduction was performed using IRAF¹ and SDFRED2 (Ouchi et al. 2004) with the following processes: overscan subtraction, flat fielding, distortion correction, sky background subtraction, and relative photometry. We estimate the flux via aperture photometry using the APPHOT task of IRAF. The aperture radius is 1.4 times that of a typical FWHM on a night that is optimum to obtain high S/N data for a point source (Howell 1992). We select 9–10 background point sources listed in the USNO-B1.0 catalog (Monet et al. 2003) as reference stars. Those are required to be brighter than 19 mag in R -band with $B - R$ of $0.90\text{--}1.04$ mag. The color range corresponds to ± 0.03 mag from $V - R = 0.44$ mag for Nereid (Schaefer and Schaefer 2000) using the color correlation of main sequence stars (Drilling and Landolt 2000). The light curves are given by the relative flux of Nereid to their total flux at each shot. The photometric accuracy reaches $0.001\text{--}0.002$ mag. The relative sensitivity among CCDs is corrected using the Sloan Digital Sky Survey (SDSS) photometric database (Abazajian et al. 2009). We have confirmed a linear correlation of magnitude between the Suprime-Cam VR -band and SDSS r -band.

Three fields at different airmass including the 4–7 Landolt standard stars with different $V - R$ colors (Landolt 2009) were taken each night. The coefficients of atmospheric extinction at Nereid’s color, namely $V - R = 0.44$ mag, are measured. The photometric zero point is estimated by V magnitude of the standard stars with airmass and color corrections. It allows VR -band flux to be converted into V -band magnitude.

3. RESULTS

The calibrated photometric measurements are presented in Table 2. The apparent magnitude of Nereid is derived from the relative flux to the reference stars and their total V magnitude. The brightness variation of a rotating body with such a small amplitude could be attributed to the changes in the cross-section area and/or albedo inhomogeneity. If Nereid is an ellipsoidal body with a constant albedo over the surface, it produces a double-peaked sinusoidal lightcurve. Indeed, Grav et al. (2003) show that a simple sinusoid model gives a good fit to Nereid’s lightcurve. We assume that Nereid is covered by surface with a uniform albedo and

¹ IRAF is distributed by the National Optical Astronomy Observatories (NOAO).

its lightcurve is doubly periodic.

For determination of the lightcurve, a variation of the observed magnitude (m_{obs}) due to the heliocentric distance (r in AU) and geocentric distance (Δ in AU) must be corrected. We use standardized magnitude (m) derived from $m_{\text{obs}} - 5\log_{10}[r\Delta/900]$. The rotational periodicity is analyzed by a Fourier-transform method called the Lomb-Scargle periodogram (Lomb 1976; Scargle 1982). The lightcurve model is represented as a first-order Fourier series formulation. In addition, we approximated the opposition effect as linear increasing with approaching the opposition.

The synthetic lightcurve with a period P to be fitted is

$$m(t) = \frac{A_c}{2} \cos(\omega(t - t_0)) + \frac{A_s}{2} \sin(\omega(t - t_0)) + k\alpha + m_0, \quad (1)$$

where t , ω , α , k , m_0 are the observed time, frequency ($\omega = 2\pi/P$), solar phase angle, slope of the phase curve, and basement magnitude, respectively. The peak-to-peak amplitude A is given by the coefficients A_c and A_s as $A = \sqrt{A_c^2 + A_s^2}$. The time epoch t_0 is evaluated by

$$\tan(2\omega t_0) = \frac{\sum_{i=1}^N \sin(\omega t_i)}{\sum_{i=1}^N \cos(\omega t_i)}, \quad (2)$$

where N is the number of data points.

We obtained a best-fit model with $P = 5.75 \pm 0.05$ hr, $A = 0.031 \pm 0.001$ mag, and $k = 0.138 \pm 0.002$ mag deg $^{-1}$. The mean residual of the fitting is 0.0026 mag, which is comparable to the photometric errors. Figure 1 shows the lightcurve combined with all the data points corrected for the opposition effect and the best-fit model folded with the oscillation period P . The rotation period ($2P = 11.50$ hr ± 0.10 hr) and amplitude (0.031 ± 0.001 mag) well agree with those presented by Grav et al. (2003), namely 11.52 ± 0.14 hr and 0.029 ± 0.003 mag. This represents the constancy of Nereid's rotation state among August 2001, August 2002 (Grav et al. 2003), and September 2008 (this study). We found no evidence of the rotation variability over 7 years. The rotation period is much shorter than the lower bound to induce the spin-orbit resonance or chaotic rotation, about 2 weeks (Dobrovolskis 1995). Nereid is observed to be and likely to remain in a constant rotation state.

Under the assumption of albedo homogeneity, the brightness fluctuation with 0.03-mag amplitude constrains the body shape. A triaxial ellipsoid with semi-axes $a \geq b \geq c$ rotating about the c axis draws a lightcurve with amplitude of

$$A = 2.5 \log \left(\frac{\bar{a}^2 \cos^2 \theta + \bar{a}^2 \bar{c}^2 \sin^2 \theta}{\bar{a}^2 \cos^2 \theta + \bar{c}^2 \sin^2 \theta} \right)^{1/2}, \quad (3)$$

where $\bar{a} = a/b$, $\bar{c} = c/b$, and θ is an aspect angle between the line of sight and the spin axis (Lacerda and Luu 2003). Given a simple prolate spheroid (*i.e.* $\bar{c} = 1$), $\bar{a} < 2.0$ in $\theta > 15^\circ$.

For a prolate body, the period of precession derived from tidal torque is represented by

$$P_{\text{pre}} \leq \frac{4(1 - e^2)^{3/2}}{3(\bar{a} - 1)} \frac{P_{\text{orb}}^2}{P_{\text{rot}}}, \quad (4)$$

where P_{pre} , P_{orb} , and P_{rot} are periods of the precession, orbit, and rotation, respectively (Dobrovolskis 1995; Schaefer et al. 2008). It is already known that Nereid has $e = 0.75$, $P_{\text{orb}} = 360.13$ days, and $P_{\text{rot}} = 0.48$ days (11.5 hr). Schaefer et al. (2008) suggest that Nereid’s precessional period is ~ 8 or ~ 16 years. Assuming $P_{\text{pre}} = 16$ years, the body must have $\bar{a} \geq 4.3$. This elongated shape is hardly acceptable to reproduce a small lightcurve amplitude, supporting the assertion that Nereid has a non-chaotic rotation with no precession.

It is widely known that atmosphereless bodies exhibit an exponential increase in reflectance at tiny solar phase angle, called an opposition surge. Schaefer et al. (2008) determined the phase curves of Nereid using multi-year-combined photometric data on 246 nights from 1998 to 2006 (see also Schaefer and Schaefer 2000; Schaefer and Tourtellotte 2001). They have a sharp brightening exceeding 0.3 mag deg^{-1} down from $\alpha \sim 0.5^\circ$, represented by the best-fit model for surface scattering (Hapke 2002) as

$$m = 19.655 - 2.5 \log_{10} \left\{ 1 + 0.54 [1 + (1 - e^{-z})/z] / [2(1 + z)^2] \right\}, \quad (5)$$

$$z = \tan[\alpha/2] / 0.0134. \quad (6)$$

On the other hand, Grav et al. (2003) reported the surge slope of $0.14 \pm 0.08 \text{ mag deg}^{-1}$ at $\alpha \sim 0.4^\circ$, which disagrees with the measurements by Schaefer et al. (2008).

Figure 2 shows the combined phase curves and their slopes of Nereid presented by this work and those of previous studies. Both the magnitude and surge slope of our data are consistent with the model curve of Eq.(5). In contrast, the surge given by Grav et al. (2003) is too shallow. The discrepancy is most likely due to the small range of phase angles spanned by their observations (0.35° – 0.46°). There is no doubt that Nereid has a steep opposition surge, indicating that the coherent backscattering mechanism is dominant on Nereid’s surface (Schaefer et al. 2008).

4. DISCUSSION

From the large, eccentric, and inclined orbit of Nereid, it is natural to consider its origin as a captured body from outside the Neptune system. Nesvorný et al. (2007) investigated the capture of irregular satellites in the planetesimal disk by three-body gravitational reactions during encounters between the giant planets. This model well reproduces the orbits of Nereid and most Neptunian irregular satellites. Also, the long-term dynamical stability of Nereid’s orbit has been confirmed (Holman et al. 2004). It is perfectly possible that Nereid has been an irregular satellite since it started orbiting around Neptune.

Suetsugu et al. (2011) found that long-lived temporary capture of planetesimals in the prograde direction occurs at a limited range of initial orbital elements. The capture rate has a peak at $\tilde{e} \simeq 3$ and $E \simeq 0$. Here, \tilde{e} is the initial orbital eccentricity scaled by $h = R_{\text{H}}/a$, where R_{H} is the Hill radius and a is the semi-major axis of the planet; E is the energy integral described as $E = (\tilde{e}^2 + \tilde{i}^2)/2 - 3\tilde{b}^2/8 + 9/2$, where \tilde{i} is the initial orbital inclination scaled by h and \tilde{b} is

the difference in the initial semi-major axis between the planet and a planetesimal scaled by R_H (Nakazawa et al. 1989). For Neptune, these conditions correspond to $e \simeq 0.08$ and $b \simeq 3.8\text{--}4.6$ AU in \tilde{i} ranging from 0 to \tilde{e} (e and b are non-scaled \tilde{e} and \tilde{b} , respectively). The source of Neptunian irregular satellites with prograde orbits is likely to be a planetesimal population in the region between 25 AU and 35 AU if they were captured at the current location of Neptune.

Although most planetesimals were lost from such a region, a portion of them possibly survives as TNOs and Centaurs. After dissipation of the disk gas, the giant planets underwent orbital migration due to angular momentum exchange with residual planetesimals (Hahn and Malhotra 1999; Tsiganis et al. 2005). This led to extensive outward transport of planetesimals from 25–35 AU to the Kuiper belt (Gomes 2003; Levison and Morbidelli 2003). Levison and Morbidelli (2003) indicate that small bodies in the entire Kuiper belt were formed within ~ 35 AU and were transported outward as a result of Neptune’s migration. Combining those studies, prograde irregular satellites of Neptune may have the same origin as TNOs and Centaurs. If Nereid derives from a captured planetesimal, this implication applies to it as well.

It is worth comparing Nereid with TNOs and Centaurs in term of some physical properties to examine this hypothesis. Nereid has optical colors of $B - V = 0.71 \pm 0.04$ mag, $V - R = 0.44 \pm 0.03$ mag, and $V - I = 0.72 \pm 0.05$ mag (Schaefer and Schaefer 2000). The colors of 351 TNOs/Centaurs are provided by the MBOSS color database² (Hainaut and Delsanti 2002). We use only those with uncertainties less than 0.05 mag for a comparison with Nereid. Figure 3 and 4 show the color-color diagrams, $B - V$ vs. $V - R$ and $B - V$ vs. $V - I$, respectively. One can see that Nereid is indistinguishable from TNOs/Centaurs in the color-color planes, supporting a common origin between them. It is notable that Nereid’s colors are similar to those of neutrally colored bodies rather than red bodies. Brown et al. (2011) suggest that TNOs formed in the inner part of the primordial disk retain H_2O , CO_2 and poor hydrocarbon species on the surface which lead to a neutral color due to UV and high-energy particle irradiation. Nereid may have been originally formed at the region inside of ~ 20 AU and transported into near Neptune’s orbit.

We also focus on the distribution of rotation period as another indicator of similarity between Nereid and TNOs/Centaurs. The rotation properties of small bodies, excluding tidally locked satellites, are dominantly changed by mutual collisions (e.g. Harris 1979). The collisional evolution of rotation period depends on the size distribution, impact velocity, and bulk density, which are unique among small-body populations. Therefore, small-body populations with the same source are expected to have a common rotation distribution.

Interestingly, TNOs/Centaurs seem to have a characteristic pattern in the size-rotation distribution. Larger bodies rotate more slowly if they are greater than a few hundred kilometers in diameter (Sheppard et al. 2008). We evaluate the probability of this trend using a large lightcurve database of 102 TNOs/Centaurs compiled by Duffard et al. (2009). Figure 5 shows

² Minor Bodies in the Outer Solar System (<http://www.eso.org/~ohainaut/MBOSS>).

the distribution of their rotation periods against diameter derived by an assumed albedo of 0.1. There appears to be a monotonic increasing trend beyond 200–300 km. We calculated the Spearman’s rank correlation coefficient (Spearman 1904; Zar 1972) of the sample including 33 objects with $D \geq 250$ km except for the tidally locked Pluto-Charon binary and Haumea, a rapidly rotating dwarf planet. The correlation coefficient is $r_s = 0.53$, meaning that large TNOs/Centaurs have a positive correlation between rotation and size at the significance level greater than 99.5 %. This trend is explained by the random accumulation effect of angular momentum through collisions (Harris 1979; Dobrovolskis and Burns 1984).

The rotation period of Nereid is plotted on Figure 5. We found that Nereid perfectly agrees with the size-rotation correlation of TNOs/Centaurs. This agreement supports the idea that Nereid and TNO/Centaur populations share the same origin. The capture scenario needs no additional spin-change events to explain the present rapid rotation, unlike the other hypothesis based on the outward ejection from nearby Neptune. It is more likely that Nereid is derived from a captured body rather than a primordial satellite of Neptune.

5. CONCLUSIONS

We present highly accurate lightcurves of Nereid on two consecutive nights and one night after one month later in September 2008 at phase angles of 0.5° – 1.3° . The periodic analysis shows that the rotation period of 11.5 ± 0.1 hr, peak-to-peak amplitude in brightness variation of 0.031 ± 0.001 mag. They completely agree with the measurements in Grav et al. (2003). On the other hand, the steepness of magnitude increases due to the opposition surge is 0.138 ± 0.002 mag deg $^{-1}$ which is consistent with the phase curve model presented by Schaefer et al. (2008). The conclusions of this work can be summarized as follows:

1. The period and amplitude of Nereid’s rotation are constant in 2001–2002 and 2008. We found no evidence of variability of the rotation state. The rapid rotation with a period much shorter than 2 weeks also rejects the chaotic rotation state suggested by Dobrovolskis (1995). These facts indicate that Nereid has a stable rotation without a tidal despinning effect.
2. Long-lived prograde captures of planetesimals by planets occur in a narrow range of the initial eccentricity and orbital energy (Suetsugu et al. 2011). If Nereid was a body captured from a heliocentric orbit, the source region is likely to be from ~ 25 AU to ~ 35 AU where it is suggested that TNOs have been formed (Gomes 2003; Levison and Morbidelli 2003).
3. The optical colors of Nereid are consistent with those of TNOs/Centaurs. Also, Nereid accords closely with the size-rotation distribution of TNOs/Centaurs. The available observations support the hypothesis that Nereid derived from a captured body and shares a common origin with the TNO/Centaur population.

We thank David Jewitt for helpful comments. This study is based in part on data

collected at Subaru Telescope. T. Terai was supported by the Grant-in-Aid from Japan Society for the Promotion of Science (20-4879).

References

- Abazajian, K. N., Adelman-McCarthy, J. K., Agüeros, M. A., et al, 2009, *ApJS*, 182, 543
- Alexander, S. G., Hesselbrock, A. J., Wu, T., Marshall, M. D., Abel, N. P, 2011, *AJ*, 142, 1
- Bailey, J. M. 1971, *Science*, 173, 812
- Brown, M. E., Schaller, E. L., Fraser, W. C, 2011, *ApJL*, 739, L60
- Brown, M. J. I., Webster, R. L. 1998, *PASA*, 15, 325
- Buratti, B. J., Goguen, J. D., Mosher, J. A. 1997, *Icarus*, 126, 225
- Dell’Oro, A., Marzari, F., Paolicchi, P., Vanzani, V, 2001, *A&A*, 366, 1053
- Dobrovolskis, A. R., Burns, J. A. 1984, *Icarus*, 57, 464
- Dobrovolskis, A. R. 1995 *Icarus*, 118, 181
- Drilling, J. S., Landolt, A. U, 2000, in *Allen’s Astrophysical Quantities*, ed. A. N. Cox (AIP Press, New York) 381
- Duffard, R., Ortiz, J. L., Thirouin, A., Santos-Sanz, P., Morales, N, 2009, *A&A*, 505, 1283
- Goldreich, P., Murray, N., Longaretti, P. Y., Banfield, D. 1989, *Science*, 245, 500
- Gomes, R. S, 2003, *Icarus*, 161, 404
- Grav, T., Holman, M. J., Kavelaars, J. J, 2003, *ApJ*, 591, L71
- Hahn, J. M., Malhotra, R. 1999, *AJ*, 117, 3041
- Hainaut, O. R., Delsanti, A. C, 2002, *A&A*, 389, 641
- Hapke, B, 2002, *Icarus*, 157, 523
- Harris, A. W. 1979, *Icarus*, 40, 145
- Holman, M. J., Kavelaars, J. J., Grav, T., Gladman, B. J., Fraser, W. C., Milisavljevic, D., Nicholson, P. D., Burns, J. A., Carruba, V., Petit, J.-M., Rousselot, P., Mousis, O., Marsden, B. G., Jacobson, R. A, 2004, *Nature*, 430, 865
- Howell S. B. 1992, in *ASP Conference Series*, Vol. 23, ed. S. B. Howell (ASP, San Francisco) 105
- Jacobson, R. A, 2009, *AJ*, 137, 4322
- Klavetter, J. J. 1989, *AJ*, 97, 570
- Lacerda, P., Luu, J, 2003, *Icarus*, 161, 174.
- Landolt, A. U., 2009, *AJ*, 137, 4186
- Levison, H. F., Morbidelli, A, 2003, *Nature*, 426, 419
- Lomb, N. R. 1976, *ASS*, 39, 447
- Mosqueira, I., Estrada, P. R, 2003, *Icarus*, 163, 198
- Miyazaki, S., Komiyama, Y., Sekiguchi, M., Okamura, S., Doi, M., Furusawa, H., Hamabe, M., Imi, K., Kimura, M., Nakata, F., Okada, N., Ouchi, M., Shimasaku, K., Yagi, M., Yasuda, N. 2002, *PASJ*, 54, 833
- Monet, D. G., Levine, S. E., Canzian, B., et al, 2003, *AJ*, 125, 984
- Nakazawa, K., Ida, S., Nakagawa, Y. 1989, *A&A*, 220, 293
- Nesvorný, D., Vokrouhlický, D., Morbidelli, A, 2007, *AJ*, 133, 1962

- Ouchi, M., Shimasaku, K., Okamura, S., Furusawa, H., Kashikawa, N., Ota, K., Doi, M., Hamabe, M., Kimura, M., Komiyama, Y., Miyazaki, M., Miyazaki, S., Nakata, F., Sekiguchi, M., Yagi, M., Yasuda, N, 2004, *ApJ*, 611, 660
- Pravec, P., Harris, A. W., Michalowski, T, 2002, in *Asteroids III*, ed. W. F. Bottke Jr., A. Cellino, P. Paolicchi, and R. P. Binzel (University of Arizona Press, Tucson) 113
- Rabinowitz, D. L., Schaefer, B. E., Tourtellotte, S. W, 2007, *AJ*, 133, 26
- Scargle, J. D. 1982, *ApJ*, 263, 835
- Schaefer, M. W., Schaefer, B. E. 1988, *Nature*, 333, 436
- Schaefer, B. E., Schaefer, M. W, 2000, *Icarus*, 146, 541
- Schaefer, B. E., Tourtellotte, S. W, 2001, *Icarus*, 151, 112
- Schaefer, B. E., Tourtellotte, S. W., Rabinowitz, D. L., Schaefer, M. W, 2008, *Icarus*, 196, 225
- Sheppard, S. S., Lacerda, P., Ortiz, J. L, 2008, in *The Solar System Beyond Neptune*, ed. M. A. Barucci, H. Boehnhardt, D. P. Cruikshank, and A. Morbidelli (University of Arizona Press, Tucson) 129
- Spearman, C. 1904, *American Journal of Psychology*, 15, 72
- Suetsugu, R., Ohtsuki, K., Tanigawa, T, 2011, *AJ*, 142, 200
- Thomas, P., Veverka, J., Helfenstein, P. 1991, *J. Geophys. Res.*, 96, 19,253
- Tsiganis, K., Gomes, R., Morbidelli, A., Levison, H. F, 2005, *Nature*, 435, 459
- Williams, I. P., Jones, D. H. P., Taylor, D. B. 1991, *MNRAS*, 250, 1P
- Wisdom, J., Peale, S. J., Mignard, F. 1984, *Icarus*, 58, 137
- Zar, J. H. 1972, *Journal of the American Statistical Association*, 67, 578

Table 1. Time-series photometric observations for Nereid.

Date (UT)	RA2000	Dec2000	r^* (AU)	Δ^\dagger (AU)	α^\ddagger (deg)	T_{obs}^\S (hour)	Number of usable images
2008 Sep 01	21 ^h 39 ^m .4	-14°22'3	30.02	29.05	0.55	1.05	14
2008 Sep 02	21 ^h 39 ^m .3	-14°22'8	30.02	29.06	0.58	2.15	26
2008 Sep 29	21 ^h 37 ^m .0	-14°34'6	30.01	29.29	1.34	1.61	22

* Heliocentric distance.

† Geocentric distance.

‡ Phase angle.

§ Time length of the observation.

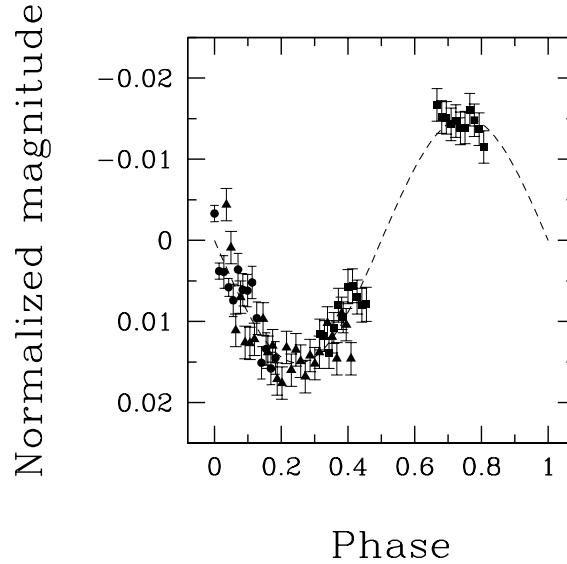


Fig. 1. Composite lightcurve of Nereid with a period of 5.75 hr. The vertical axis shows normalized magnitude corrected for the opposition effect. The circles, triangles and squares represent the data obtained on 2008 September 1, 2, and 29, respectively. The dashed curve is the best-fit model with a peak-to-peak amplitude of 0.031 mag.

Table 2. Photometric measurements of Nereid.

MJD*	Airmass	m_V^{\dagger} (mag)
54710.2722	1.64	19.367 ± 0.001
54710.2755	1.61	19.374 ± 0.001
54710.2789	1.58	19.374 ± 0.002
54710.2823	1.55	19.376 ± 0.001
54710.2857	1.52	19.378 ± 0.002
54710.2891	1.50	19.374 ± 0.002
54710.2925	1.47	19.377 ± 0.002
54710.2959	1.45	19.377 ± 0.002
54710.2992	1.43	19.376 ± 0.002
54710.3026	1.41	19.380 ± 0.002
54710.3059	1.39	19.386 ± 0.002
54710.3093	1.37	19.384 ± 0.002
54710.3127	1.36	19.386 ± 0.002
54710.3160	1.34	19.385 ± 0.002
54711.2394	2.06	19.370 ± 0.002
54711.2427	2.00	19.376 ± 0.002
54711.2461	1.94	19.386 ± 0.002
54711.2495	1.89	19.382 ± 0.002
54711.2529	1.84	19.388 ± 0.002
54711.2563	1.79	19.388 ± 0.002
54711.2596	1.75	19.387 ± 0.002
54711.2658	1.68	19.385 ± 0.002
54711.2692	1.64	19.389 ± 0.002
54711.2726	1.61	19.388 ± 0.002
54711.2759	1.58	19.392 ± 0.002
54711.2793	1.55	19.393 ± 0.002
54711.2826	1.52	19.388 ± 0.002
54711.2860	1.50	19.391 ± 0.002
54711.2893	1.48	19.389 ± 0.002
54711.2927	1.45	19.390 ± 0.002
54711.2961	1.43	19.392 ± 0.002
54711.2995	1.41	19.389 ± 0.002
54711.3029	1.39	19.390 ± 0.002
54711.3062	1.38	19.389 ± 0.002
54711.3120	1.35	19.385 ± 0.002

Table 2. (Continued.)

MJD*	Airmass	m_V^\dagger (mag)
54711.3153	1.33	19.387 ± 0.002
54711.3187	1.32	19.390 ± 0.002
54711.3221	1.31	19.384 ± 0.002
54711.3255	1.30	19.386 ± 0.002
54711.3289	1.29	19.390 ± 0.002
54738.2333	1.37	19.480 ± 0.002
54738.2367	1.35	19.481 ± 0.002
54738.2400	1.34	19.482 ± 0.002
54738.2434	1.32	19.482 ± 0.002
54738.2468	1.31	19.482 ± 0.002
54738.2501	1.30	19.483 ± 0.002
54738.2535	1.29	19.483 ± 0.002
54738.2568	1.28	19.481 ± 0.002
54738.2601	1.27	19.482 ± 0.002
54738.2635	1.26	19.483 ± 0.002
54738.2669	1.25	19.485 ± 0.002
54738.3888	1.42	19.509 ± 0.002
54738.3922	1.44	19.509 ± 0.002
54738.3955	1.46	19.511 ± 0.002
54738.3989	1.48	19.508 ± 0.002
54738.4022	1.50	19.505 ± 0.002
54738.4056	1.53	19.507 ± 0.002
54738.4090	1.55	19.503 ± 0.002
54738.4123	1.58	19.503 ± 0.002
54738.4156	1.61	19.504 ± 0.002
54738.4190	1.65	19.505 ± 0.002
54738.4223	1.68	19.505 ± 0.002

* Modified Julian date.

† Apparent V -band magnitude.

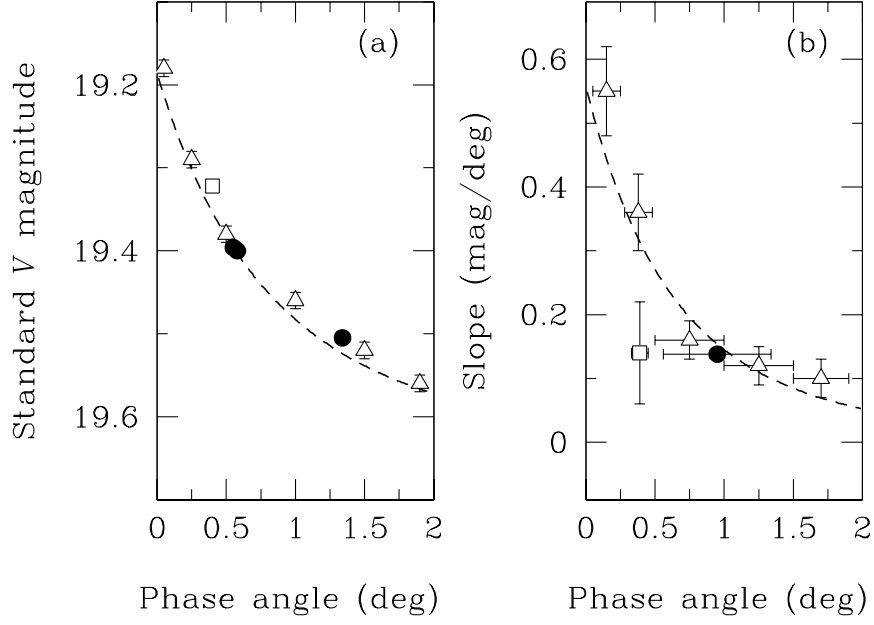


Fig. 2. (a) V-band basement magnitude of Nereid's lightcurves standardized by heliocentric/geocentric distances ($m_{\text{obs}} - 5\log_{10}[r\Delta/900]$; see text) as a function of solar phase angle. The data are derived from this work (filled circles), Schaefer et al. (2008) (open triangles), and Grav et al. (2003) (open squares). The dashed curve is the best-fit model of the opposition surge given in Schaefer et al. (2008). (b) Slopes of the measured phase curves of Nereid in mag deg^{-1} . The symbols and dashed curve are the same as (a). The horizontal bar on each point shows the range of phase angle used in estimation of the slope.

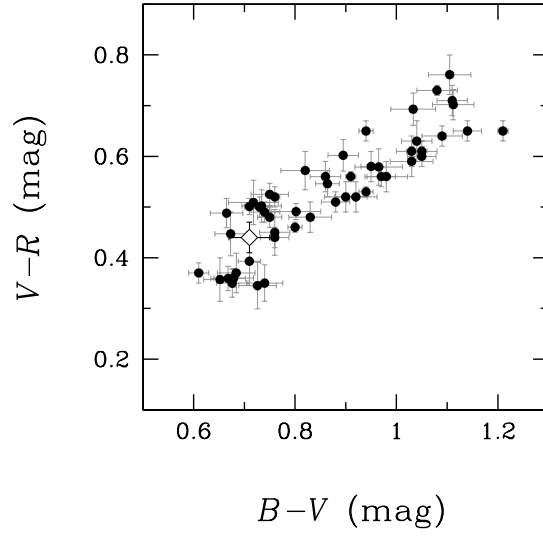


Fig. 3. Color-color diagram of $B - V$ vs. $V - R$ for Nereid (open diamond; Schaefer and Schaefer 2000) and TNOs/Centaurs (filled circles; Hainaut and Delsanti 2002).

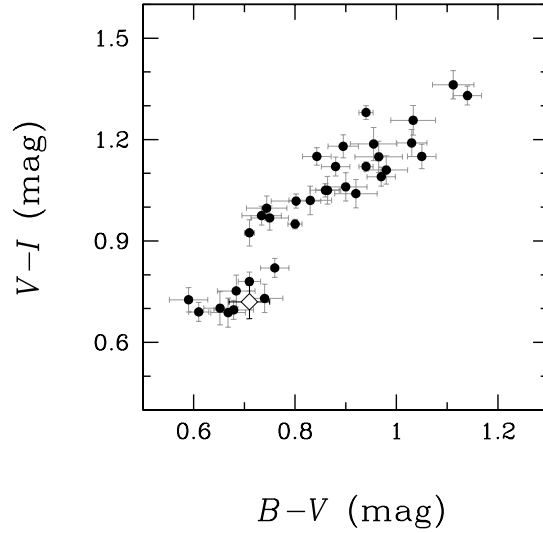


Fig. 4. Color-color diagram of $B - V$ vs. $V - I$ for Nereid (open diamond; Schaefer and Schaefer 2000) and TNOs/Centaurs (filled circles; Hainaut and Delsanti 2002).

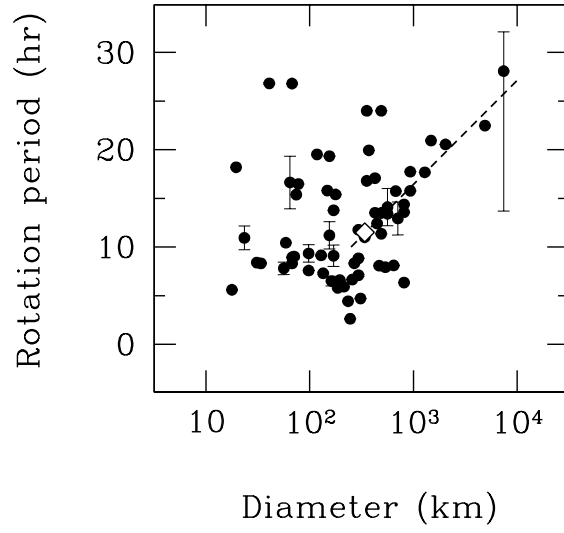


Fig. 5. The size-rotation distribution of TNOs and Centaurs presented in Duffard et al. (2009). The dashed line shows a linear regression line to the plot of $\log D$ (D is diameter) vs. rotation periods of those bodies with $D > 250$ km except for Pluto, Charon, and Haumea. An open diamond represents Nereid.